

**PSI** Center for Neutron and  
Muon Sciences

# Muonic atom spectroscopy at PSI and the development of the MIXE technique



Issa Briki (on behalf of the **MIXE** team)  
Laboratory for Muon Spin Spectroscopy (LEM group)

Huizhou, China 25-27 April 2026

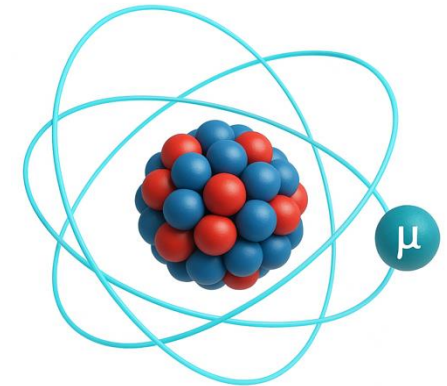
1

---

# Muonic atoms

# Introduction

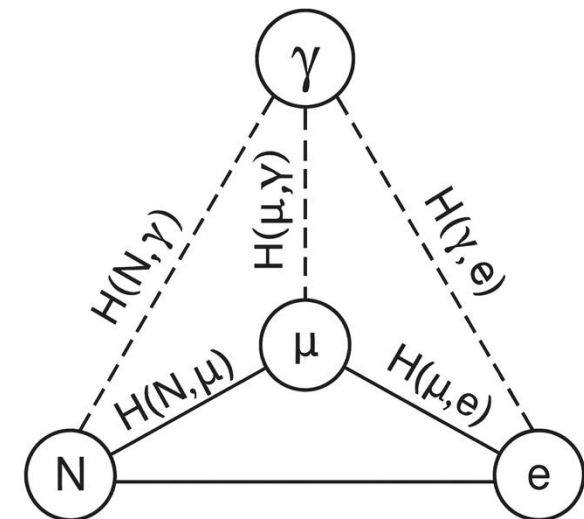
- Single negative muon bound to a single atomic nucleus.
- The physics of the muonic atom happens in a time interval of about  $10^{-14}$  s.



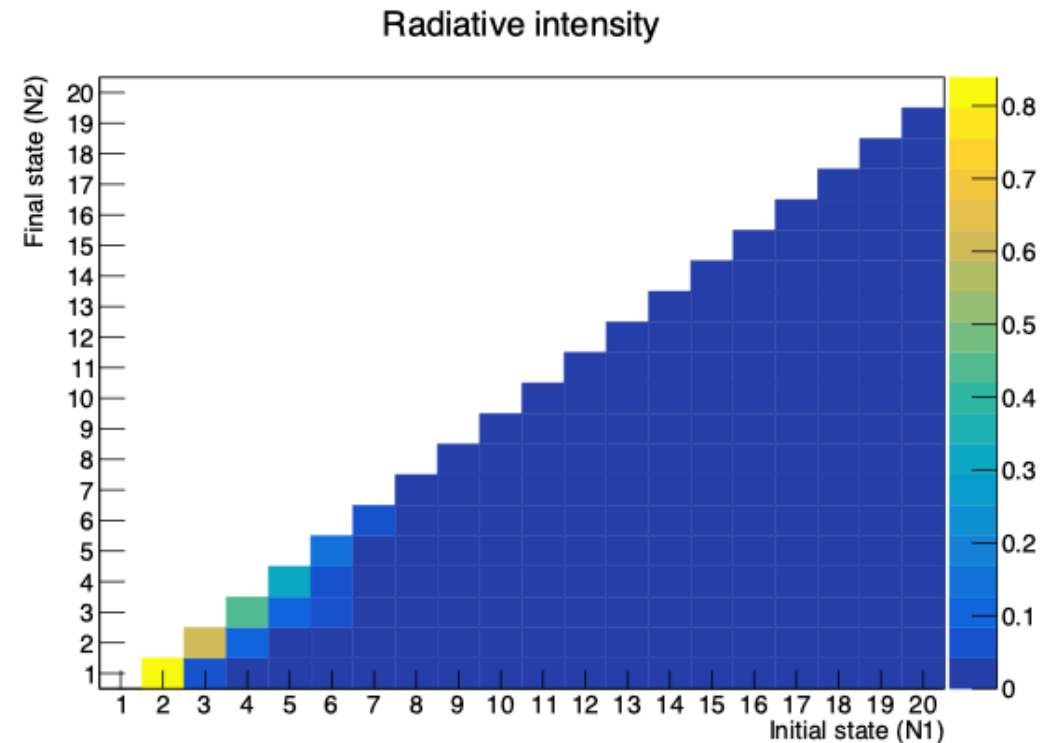
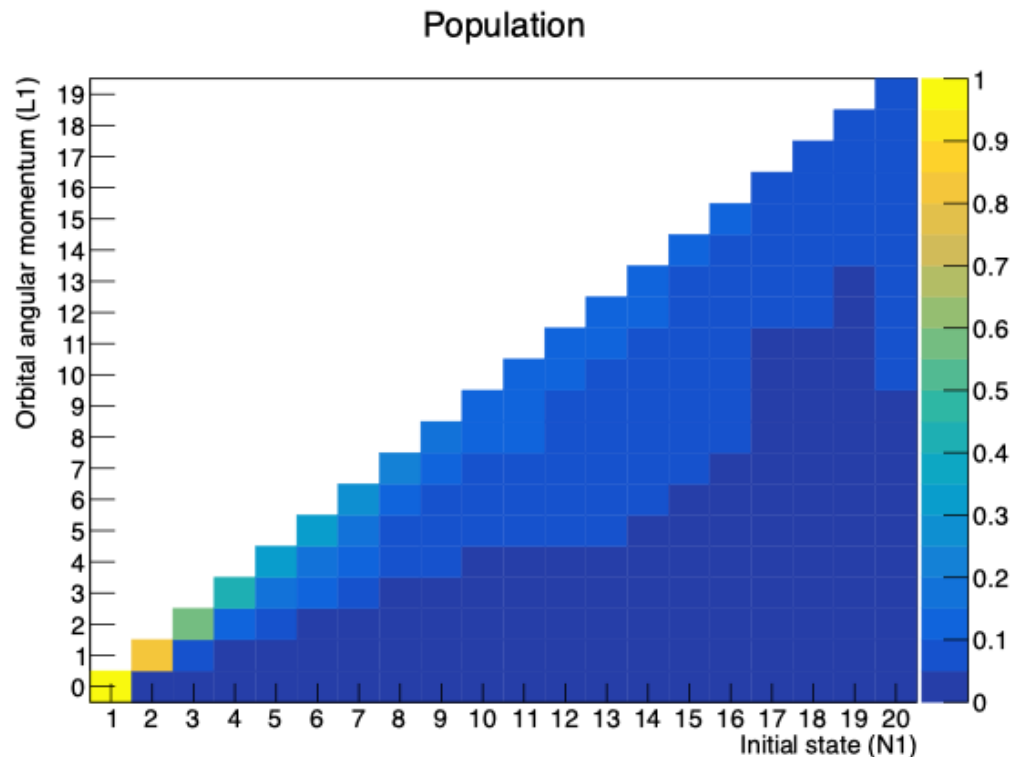
## Model Hamiltonian

The electromagnetic interactions are treated in the **Coulomb gauge**:

- The  $\mu$ ,  $e^-$ , and N interact via the static **Coulomb interaction**:  
$$H(\mu) = H(\text{free } \mu) + H(\mu, N) + H(\mu, e^-)$$
- The  $\mu$ ,  $e^-$ , and N interact with the transverse **photon field**:  
These interactions give rise to magnetic interactions between N and  $\mu$ , the emission (absorption) of gamma rays.



# Muonic cascade



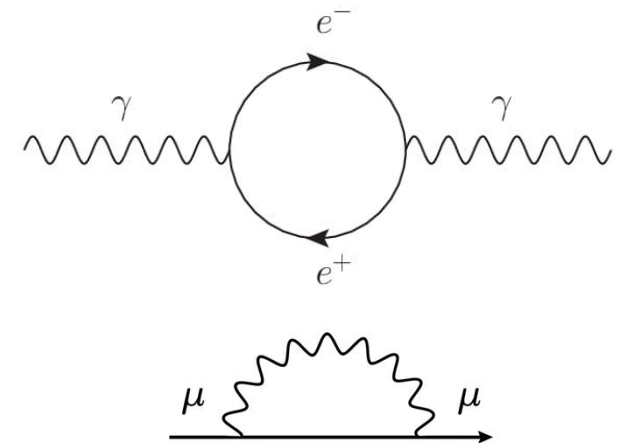
- The highest orbits ( $n > 5$ ) overlap with the electronic cloud -> **Auger transitions** dominate
- The lowest orbits ( $n < 4$ ) are close to the nucleus -> **Radiative transitions** dominate
- The refilling of holes depends on the chemical or physical environment.
- This refilling mechanism leads to observable effects on the muonic cascade.

# Muonic energy

**Finite size effect:** at proximity to the nucleus, the nuclear potential undergoes an extreme change which end in the energy shift. (reduction of about 50 % in case of  $^{75}\text{Re}$ , [Abu Saleh et al.](#))

## QED effects:

- **Vacuum polarization:** the emission of virtual  $e^-e^+$  pairs changes the nuclear potential; thus, the muon feels a larger effective charge (binding energy increases by a few 10 of keV).
- **Self-energy:** the reduction of the muon's binding energy is due to its interaction with the electromagnetic field it produces (binding energy increases by a few keV)



## Other corrections:

- **Electron screening:** the presence of the  $e^-$  decreases the effective charge experienced by the muon and thus reduce its binding energy by few eV ( $n > 5$ ).
- **Recoil effect, Orbital collapse, isotope and isomer shifts, ....**

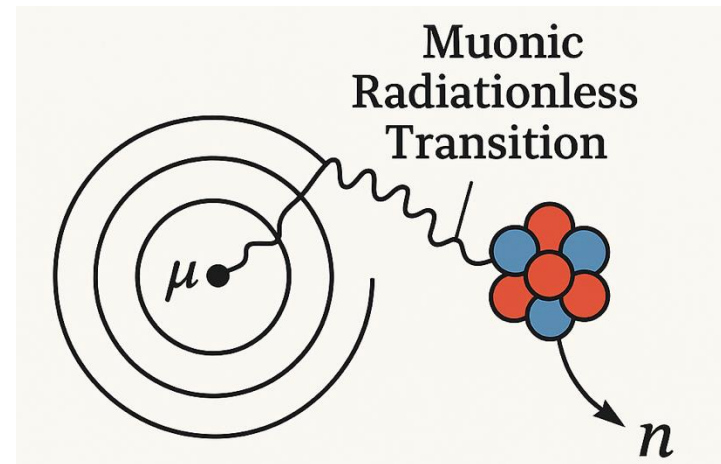
# The resonance excitation

When the energy difference between muonic levels is close to, or nearly degenerate with, a nuclear excitation energy, the muon can lead to resonance excitation of the nucleus.

- Anomalous lines of significant intensity have been observed in  $^{76}\text{Os}$  and  $^{70}\text{Yb}$  and are interpreted as 3d-2p muonic-nuclear resonance (M. V. Hoehm et al).
- This resonance may occur frequently in heavy muonic atoms (L. Wilets et al.).
- This resonance could result in the excitation of low-lying and high-lying nuclear states in certain deformed nucleus and nucleus near  $^{82}\text{Pb}$  respectively.
- (M. Y. Chen et al.) resonance excitation in  $^{81}\text{Tl}$
- (W. Y. Lee et al. 1972) (J. HUFNER) resonance excitation in  $^{83}\text{Bi}$
- (W. Y. Lee et al. 1971) (J. HUFNER) resonance excitation in  $^{53}\text{I}$
- (WILLIAM B. ROLNICK) resonance excitation in  $\text{Tl}$ ,  $\text{Pb}$ , and  $\text{Bi}$

# Nuclear Auger Effect

- The nuclear Auger transitions resemble the internal conversion process for nuclear gamma-rays, except that the roles of the nucleus and the atom are swapped.

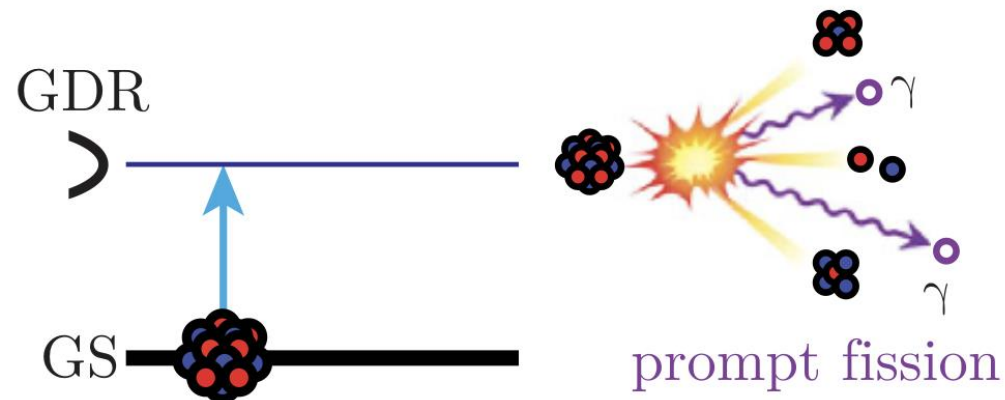



- This effect occurs (when the muonic transition energy is higher than the binding energy of the neutron) predominantly for the lowest transitions (e.g. E1, E2) and in heavy nucleus.
- The neutron is ejected at the same time scale of the muonic X-rays (both transition are electromagnetic)
- Neutron rate per stopped muon: 5% to 10% (Zaretskii et al); 7% (Hargrove et al)

# Muon-induced fission

- **Prompt fission**: immediate breakup of the nucleus after absorbs radiationless energy ( $10^{-20}$  s)
- Excited muonic atoms in the actinide region ( $Z > 88$ ) may induce prompt fission (Y. E. Oberacker et al.)
- The E2 muonic transition energy is close to the ISGOR peak of the isoscaler giant quadrupole resonance in actinide nucleus which exhibits a large fission width.

ISGOR: is a collective vibration of the nucleus where all the protons and neutrons oscillate together forming a quadrupole or a “rugby ball” Shape.




**PSI** Center for Neutron and Muon Sciences  
**MuCascade: A Database of Muonic X-ray Transition Energies and Intensities.**

Authors: Issa Briki<sup>1\*</sup>, Michael W. Heiss<sup>1</sup>, Xiao Zhao<sup>1</sup>, Maxime Lamotte<sup>1</sup>, Gianluca Janka<sup>1</sup>, and Thomas Prokscha<sup>1</sup>.  
<sup>1</sup>PSI Center for Neutron and Muon Sciences CNM, 5232 Villigen PSI, Switzerland.  
 \*Issa.briki@psi.ch

**Abstract**  
 Muonic atoms are powerful probes of atomic and nuclear structure through their characteristic X-ray transitions. Accurate modeling of these spectra requires reliable transition energies and intensities. **Cascade calculations** [1] are used to determine the transition intensities, accounting for the main physical processes governing the muonic cascade. To improve the description of transition energies, **MuDirac** [2] is used, which solves the Dirac equation including nuclear size, vacuum polarization, and electronic screening. Using these two complementary approaches, we construct a database containing cascade transition intensities and MuDirac-calculated energies for muonic atoms across a wide range of elements. The calculated transition energies and relative intensities are compared with available experimental muonic X-ray measurements.

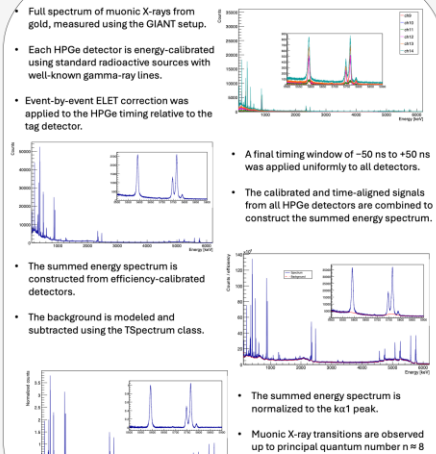
**Method**

- Transition intensities computed for  $Z = 4-103$  (up to  $n = 20$ ).
- Good agreement with experiment for dipole transitions; discrepancies remain for some quadrupole transitions.
- New C++ cascade code under validation.
- Muonic X-ray energies obtained with MuDirac for all elements and stable isotopes.
- Experiments are performed using the **GIANT** setup (Germanium Array for Non-destructive Testing) [3].



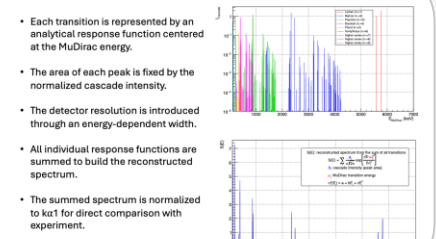
**Experimental Approach**

- Full spectrum of muonic X-rays from gold, measured using the GIANT setup.
- Each HPGe detector is energy-calibrated using standard radioactive sources with well-known gamma-ray lines.
- Event-by-event ELET correction was applied to the HPGe timing relative to the tag detector.
- A final timing window of  $-50$  ns to  $+50$  ns was applied uniformly to all detectors.
- The calibrated and time-aligned signals from all HPGe detectors are combined to construct the summed energy spectrum.
- The summed energy spectrum is constructed from efficiency-calibrated detectors.
- The background is modeled and subtracted using the TSpectrum class.
- The summed energy spectrum is normalized to the  $ka_1$  peak.
- Muonic X-ray transitions are observed up to principal quantum number  $n = 8$ .



**Computational Approach**

- Each transition is represented by an analytical response function centered at the MuDirac energy.
- The area of each peak is fixed by the normalized cascade intensity.
- The detector resolution is introduced through an energy-dependent width.
- All individual response functions are summed to build the reconstructed spectrum.
- The summed spectrum is normalized to  $ka_1$  for direct comparison with experiment.



**Conclusion**

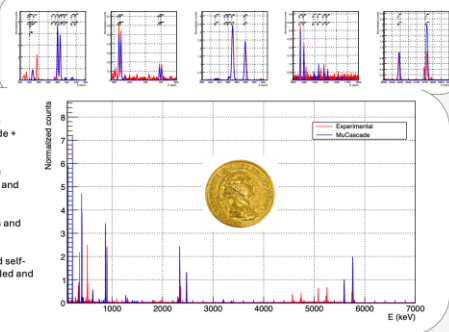
- The combined MuCascade approach provides a reliable description of muonic X-ray spectra.
- Current limitations (HF splitting, self-absorption, cascade refinements) define the next development steps.
- A validated, comprehensive database covering all the periodic table is in preparation and will be released upon completion of systematic benchmarking.

**References**

[1] V. Alyas, *Comput. Phys. Commun* 15, (1978).  
 [2] S. Sturmilo, *X-Ray Spectrometry* 50, 180 (2021).  
 [3] L. Gerchow, *Review of Scientific Instruments* 94, (2023).

**Results**

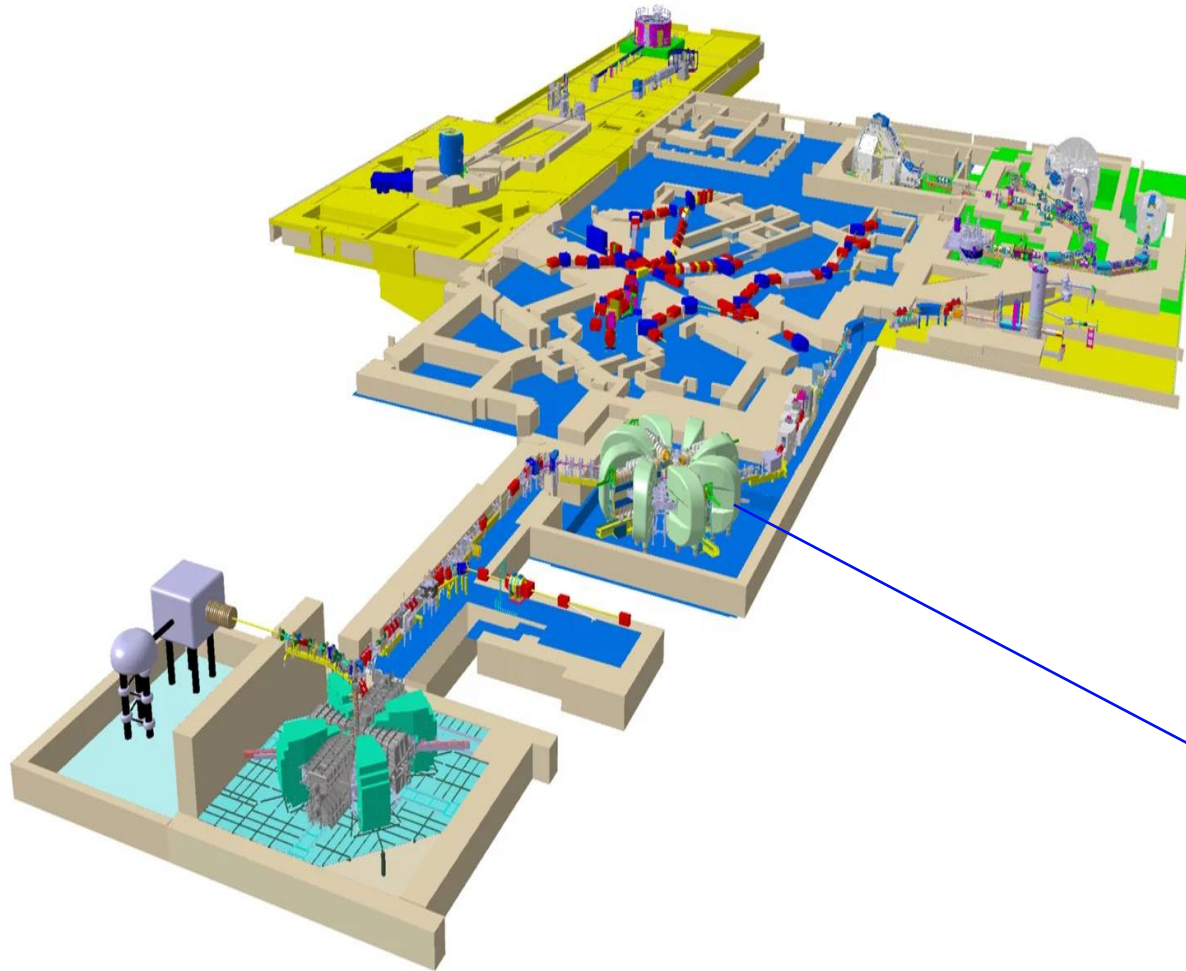
- The summed Au energy spectrum is compared with MuCascade (cascade + MuDirac).
- Good agreement is observed for the dominant transitions in both energy and relative intensity.
- Discrepancies in some weaker lines and selected transitions.
- Missing hyperfine structure (HF) and self-absorption effects are not yet included and are likely sources of the residual discrepancies.



2

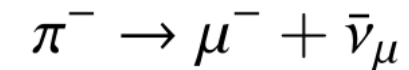
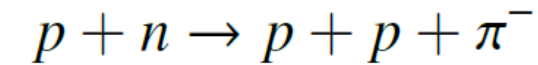
---

# Facility & Instrument

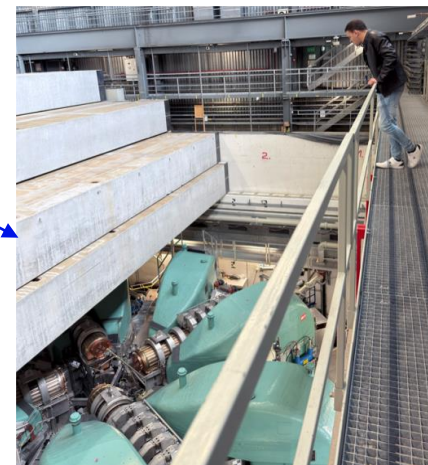


## HIPA : High Intensity Proton Accelerator

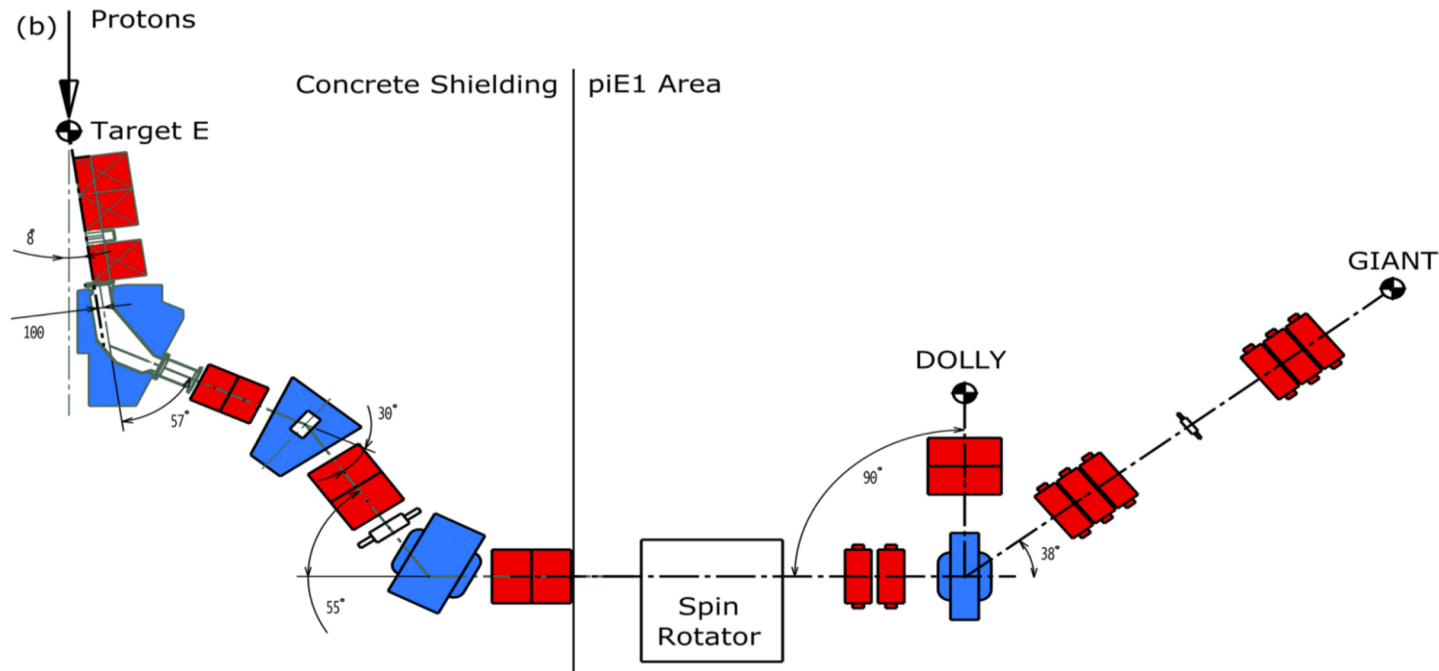
- HIPA provides  $10^{16}$  protons per second (1.4 MW).
- The proton beam is used to produce muons:



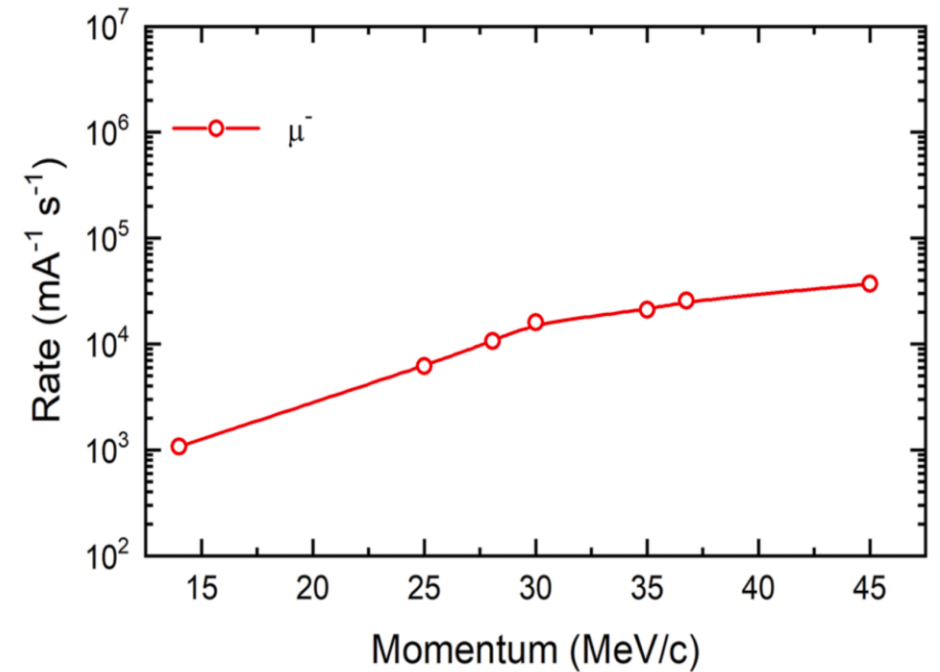
- The rest of the proton beam (60 %) is transported to a neutron spallation source (SINQ).

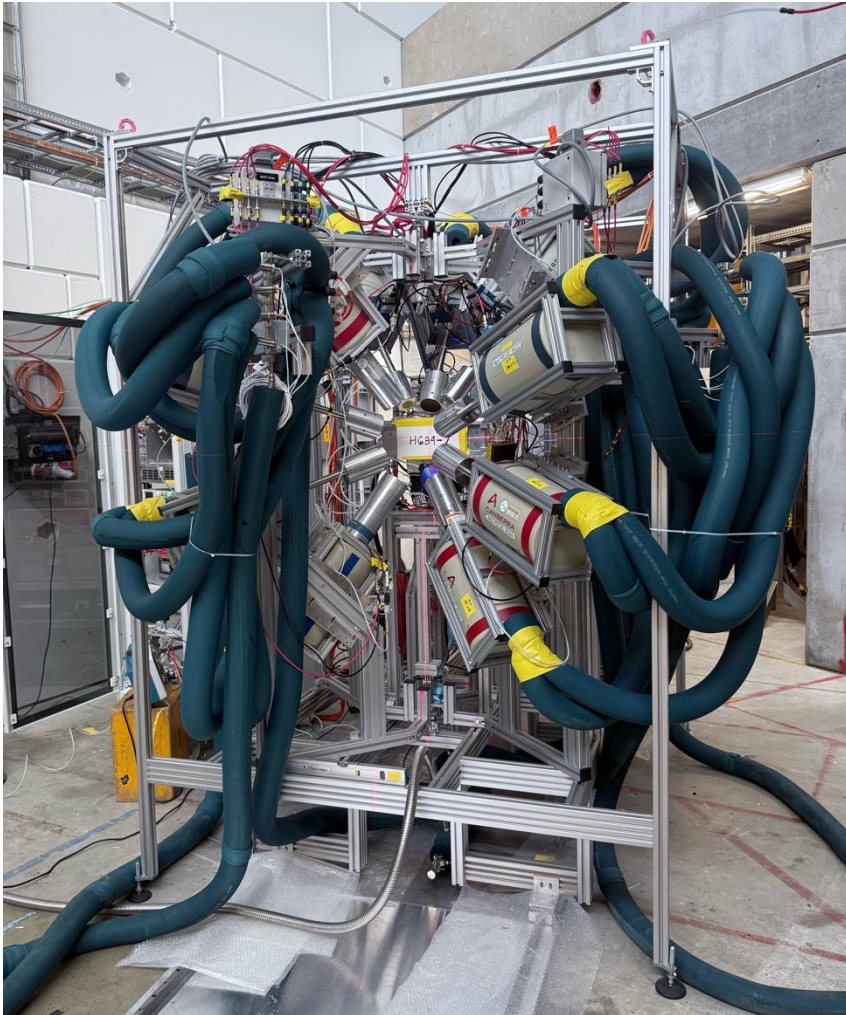


# PiE1 Beamline



- Typical  $\mu^-$  momenta : 15-60 MeV/c.
- Rates range from  $10^3$  to  $10^5$   $\mu^-$  per second on target.





L. Gerchow, et al., Germanium Array for Non-destructive Testing (GIANT) setup for muon-induced X-ray emission (MIXE) at the Paul Scherrer Institute, *Rev. Sci. Instrum.* 94 (4) (2023) 045106.

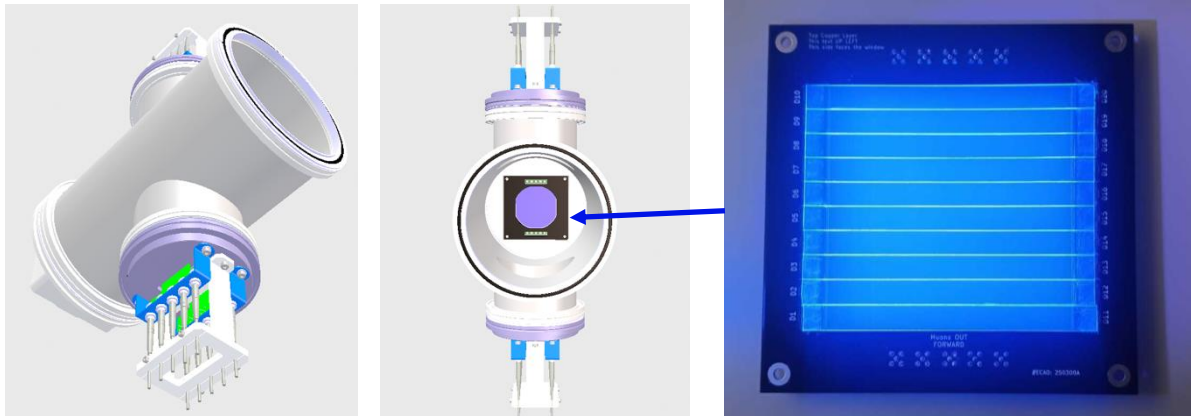
## GIANT: Germanium Array for Non-destructive Testing

- **Mechanical Structure:**
  - Aluminum Frame.
  - Fully Movable as a Unit.
- **Detector Configuration:**
  - 8 Freely Rotating Arms (*Currently 5 installed*).
  - 4 BigMac HPGe Detectors per Arm.
  - 30 HPGe Detectors Total (*Currently ~12 Installed*).
  - Reproducible positions and angles.
  - HPGe detectors shared with multiple experiments.
- **Cryogenics & Automation:**
  - Fully Automatic Liquid Nitrogen (LN<sub>2</sub>) Refill System
- **Sample Holder:**
  - A central target/sample position ensures symmetrical detector geometry for optimized detection efficiency and angular coverage.

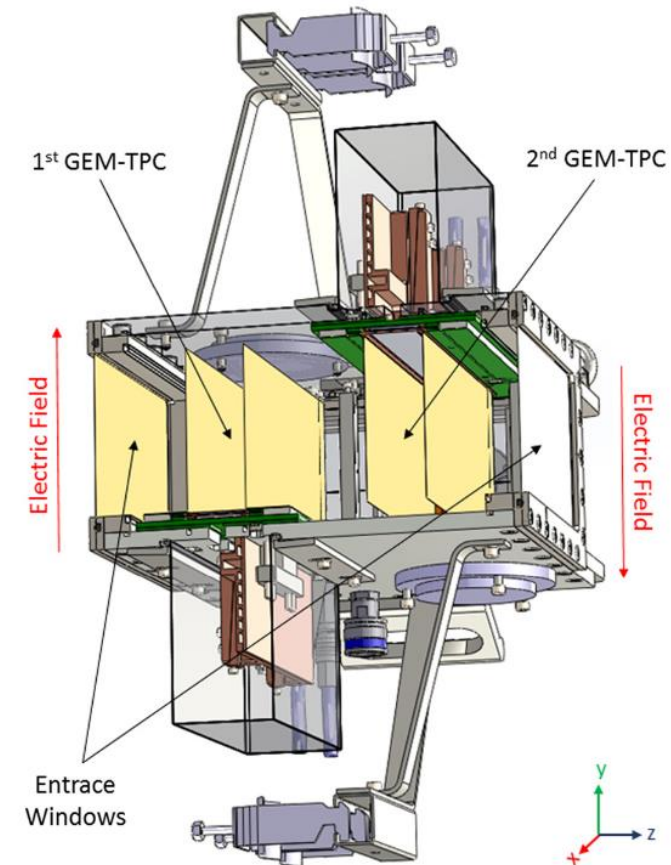
# Tagging and Tracking

## Tagger detector:

- BC-400 plastic scintillators: striped design (10 individual channels).
- Active area ( $\sim 7 \times 7 \text{ cm}^2$ ).
- Allows for discrimination of nuclear capture events.
- Reduces uncorrelated background
- Beamport:  $50 \mu\text{m}$  Mylar



## Tracker detector:



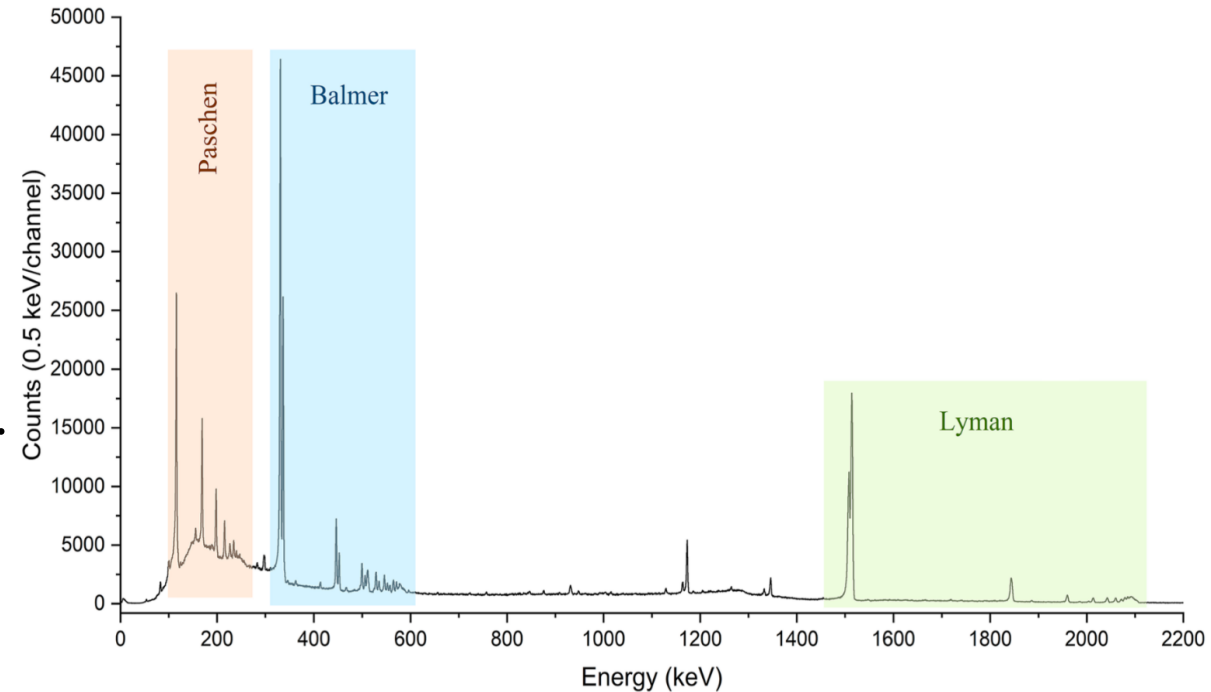
3

---

**MIXE**

# Elemental Analysis

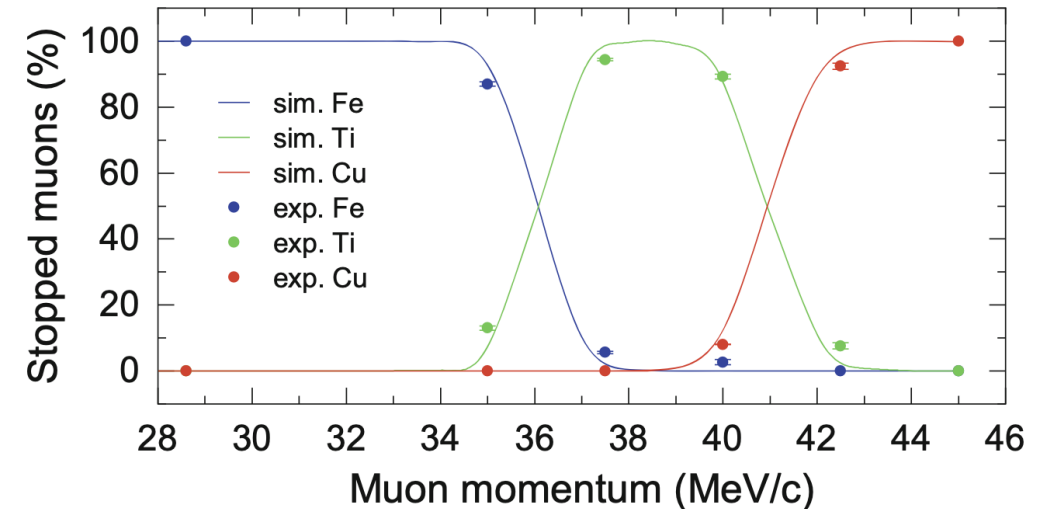
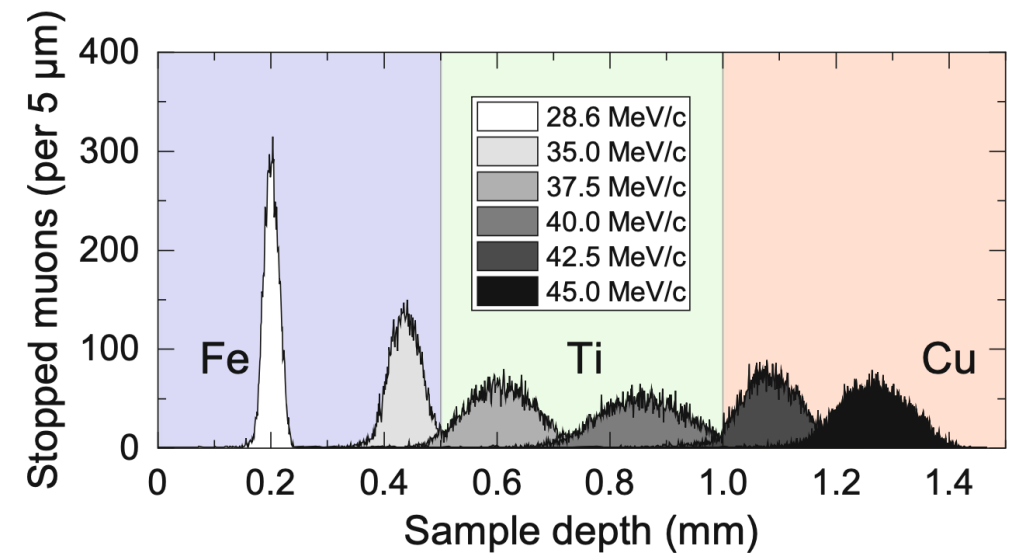
- X-ray Spectrum from Muon-Irradiated Iron Sample:
- Single HPGe detector.
- Beam momentum: 28.6 MeV/c.
- Acquisition time: 0.5 h
  
- Series lines are clearly visible in the X-ray spectrum.
- MIXE produces high-energy X-rays that travel much farther in the material.



- Compared to XRF or PIXE, MIXE's higher-energy X-rays **penetrate deeper** with **less attenuation**, enabling bulk rather than surface-only analysis.

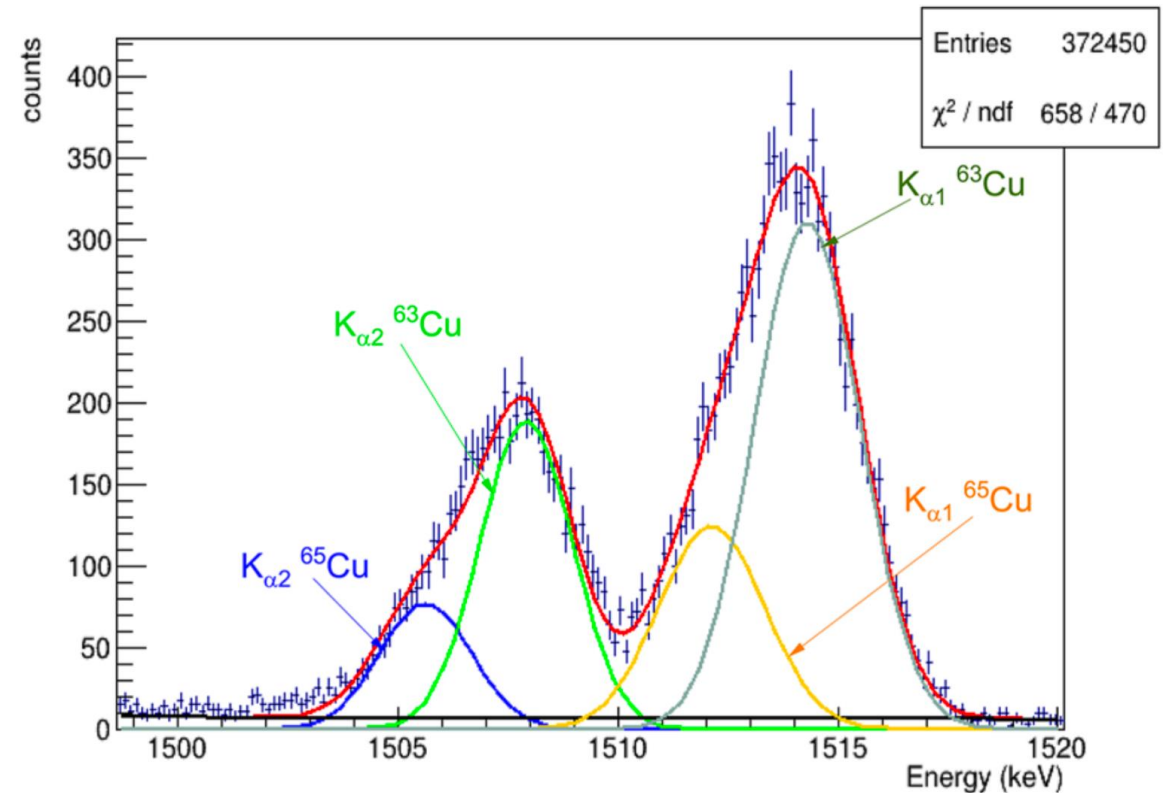
# Depth Dependence

- Simulation of the capture profiles of  $\mu^-$  in Tri-layer (thickness of each layer  $500\ \mu\text{m}$ ).
- Muon momentum tuning allows scanning of element occurrence as a function of penetration depth.
- Comparison between simulation and measured  $K_\alpha$  line intensities shows good agreement.
- Implantation depths :  $\sim\ \mu\text{m}$  to  $\sim\ \text{cm}$ .



# Isotopic composition

- The nuclear radius of isotopes of an element follows an  $A^{1/3}$  dependence.
- Nuclear polarization causes additional isotope-dependent energy shifts.
- These shifts open the possibility of determining isotopic ratios by MIXE (For  $Z \gtrsim 20$ ).
- Spectrum showing the  $K_{\alpha 1}$  and  $K_{\alpha 2}$  lines for a copper sample.



- MIXE doesn't just tell us what element is present, it can also tell us which isotope, and it can do so non-destructively and deep inside the sample.

4

---

# Conclusion

# Conclusion

- **Why MIXE:**
- MIXE is non-destructive.
- Elemental analysis, depth dependence, isotopic composition, and tomography.
- Not only archaeology, but we can also explore other samples.
- The MIXE call for proposals has been open since the beginning of this year (no cost for users).

<https://www.psi.ch/en/smus/calls>

[issa.briki@psi.ch](mailto:issa.briki@psi.ch)

- **Acknowledgement:**



**Meteorites**

**Batteries**

*and many more!*

5

---

**Backup**